Outer membrane vesicles are vehicles for the delivery of Vibrio tasmaniensis virulence factors to oyster immune cells.

Audrey Sophie Vanhove, Marylise Duperthuy, Guillaume M Charrière, Frédérique Le Roux, David Goudenège, Benjamin Gourbal, Sylvie Kieffer-Jaquinod, Yohann Couté, Sun Nyunt Wai, Delphine Destoumieux-Garzón

Environmental Microbiology (2015) vol 17 pp 1152-1165.

Outer membrane vesicles are vehicles for the delivery of *Vibrio tasmaniensis* virulence factors to oyster immune cells

Audrey Sophie Vanhove,[1,2,3,4] Marylise Duperthuy,[2,5] Guillaume M. Charrière,[1,2,3,4] Frédérique Le Roux,[6,7,8] David Goudenège,[6,7,8] Benjamin Gourbal,[9] Sylvie Kieffer-Jaquinod,[10,11,12] Yohann Couté,[10,11,12] Sun Nyunt Wai[5] and Delphine Destoumieux-Garzón[1,2,3,4]*

[1]*Ecology of Coastal Marine Systems, CNRS UMR 5119, Montpellier F-34095, France.* [2]*Ecology of Coastal Marine Systems, Ifremer, Montpellier F-34095, France.* [3]*Ecology of Coastal Marine Systems, University of Montpellier 1, Montpellier F-34095, France.*

[4]*Ecology of Coastal Marine Systems, University of Montpellier 2 and IRD, Montpellier F-34095, France.*

[5]*Department of Molecular Biology, The Laboratory for Molecular Infection Medicine Sweden (MIMS), Umeå University, Umeå S-90187, Sweden*

[6]*Unité Physiologie Fonctionnelle des Organismes Marins, Ifremer, Plouzané F-29280, France.*

[7]*Integrative Biology of Marine Models UPMC Univ Paris 06, Sorbonne Universités, Roscoff Cedex F-29688, France.*

[8]*Integrative Biology of Marine Models, CNRS UMR 8227, Station Biologique de Roscoff, Roscoff Cedex F-29688, France.*

[9]*Ecology and Evolution of Interactions, CNRS UMR 5244, Université de Perpignan Via Domitia, Perpignan Cedex F-66860, France.*

[10]*U1038, Université Grenoble-Alpes, Grenoble F-38054, France.*

[11]*iRTSV, Biologie à Grande Echelle, CEA, Grenoble F-38054, France.*

[12]*U1038, INSERM, Grenoble F-38054, France.*

Summary

Vibrio tasmaniensis LGP32, a facultative intracellular pathogen of oyster haemocytes, was shown here to release outer membrane vesicles (OMVs) both in the extracellular milieu and inside haemocytes. Intracellular release of OMVs occurred inside phagosomes of intact haemocytes having phagocytosed few vibrios as well as in damaged haemocytes containing large vacuoles heavily loaded with LGP32. The OMV proteome of LGP32 was shown to be rich in hydrolases (25%) including potential virulence factors such as proteases, lipases, phospholipases, haemolysins and nucleases. One major caseinase/ gelatinase named Vsp for vesicular serine protease was found to be specifically secreted through OMVs in which it is enclosed. Vsp was shown to participate in the virulence phenotype of LGP32 in oyster experimental infections. Finally, OMVs were highly protective against antimicrobial peptides, increasing the minimal inhibitory concentration of polymyxin B by 16-fold. Protection was conferred by OMV titration of polymyxin B but did not depend on the activity of Vsp or another OMV-associated protease. Altogether, our results show that OMVs contribute to the pathogenesis of LGP32, being able to deliver virulence factors to host immune cells and conferring protection against antimicrobial peptides.

Introduction

Characterizing the molecular bases of vibrio–host interactions is of prime importance to understand how colonization is orchestrated and persistence established (Lindell *et al*., 2012; Kremer *et al*., 2013). Oysters are naturally colonized by pathogenic and non-pathogenic vibrios, but attention has mainly been paid to pathogenic interactions. Pathogenic strains related to *Vibrio aestuarianus* or *Vibrio splendidus* have been repeatedly isolated during massive mortalities of *Crassostrea gigas* (for review, see Schmitt *et al*., 2011). Strains of *V. aestuarianus* have evolved a so-called 'outsider strategy' to promote an extracellular life cycle within the oyster by interacting specifically with oyster haemocytes (Olivot *et al*., 2006). Indeed, the haemocytes of oysters infected with the *V. aestuarianus* strain 01/32 displayed lower adhesion and phagocytosis capacities as well as increased production of reactive oxygen species (ROS) (Labreuche *et al*., 2006; 2010). On the contrary, the strain LGP32 (Gay *et al*., 2004) recently assigned to *V. tasmaniensis* within the Splendidus clade (Sawabe *et al*., 2013) was found to be a facultative intracellular pathogen that invades the oyster immune cells, the haemocytes, in which it inhibits phagosome maturation and ROS production (Duperthuy *et al*., 2011). An *ompU*-deletion mutant deficient for cell invasion was shown to be impaired in virulence, suggesting that cell invasion is required for virulence of LGP32. While mechanisms of cell invasion have been described in details, the intracellular lifestyle (intravacuolar/intracytosolic) of LGP32 remains unknown and the molecular bases of its intracellular survival and virulence are still poorly understood (Duperthuy *et al*., 2011).

Secretion of extracellular products (ECPs) is the major mechanism by which Gram-negative pathogens communicate with and intoxicate host cells (Kuehn and Kesty, 2005). ECPs of vibrios

pathogenic for marine animals have been described for their content in toxins. Among them, molecules with haemolytic, cytolytic, proteolytic and lipolytic activities have been identified (for review, see Méndez *et al*., 2012), a major attention being paid to extracellular proteolytic enzymes. Those toxic compounds required for the life cycle of microorganism are secreted by both non-pathogenic and pathogenic microorganisms. They can be lethal to the host when produced by pathogenic bacteria (Miyoshi and Shinoda, 2000). Thus, metalloproteases are important virulence factors in a broad series of human and animal diseases (Shinoda and Miyoshi, 2011). In the *V. aestuarianus* strain 01/32, ECPs were found to mediate avoidance of phagocytosis (Labreuche *et al*., 2006), to cause major damages to haemocyte *in vitro* (Labreuche *et al*., 2010) and to be toxic for oysters (Labreuche *et al*., 2006). This toxicity would be conferred by the Vam metalloprotease (Labreuche *et al*., 2010). Similarly, in *V. tasmaniensis* LGP32, the Vsm metalloprotease was found to be the main toxic factor of ECPs (Le Roux *et al*., 2007) while the contribution of the InhA/PrtV protease was minor (Binesse *et al*., 2008). Still, the major metalloprotease Vsm was not required for virulence in experimental infections (Le Roux *et al*., 2007).

ECPs have been shown to contain insoluble vesicles released from the envelope of bacteria (Deatherage *et al*., 2009). Outer membrane vesicles (OMVs), which form the insoluble fraction of Gram-negative bacteria ECPs, are extruded from the bacterial cell surface and may entrap some of the underlying periplasmic contents (Wai *et al*., 1995; Beveridge, 1999). They are actually considered as a novel secretion system in Gramnegative bacteria (Lee *et al*., 2008). OMVs can perform a variety of functions, including binding and delivery of DNA, transport of virulence factors, protection of the cell from outer membrane targeting antimicrobials and ridding the cell of toxic envelope proteins (Manning and Kuehn, 2013). Thus, they are major players in the interaction between Gram-negative bacteria and both the prokaryotic and eukaryotic cells in their environment (Kulp and Kuehn, 2010). By their transport and protective functions, they play an essential role in host–pathogen interactions (Kuehn and Kesty, 2005).

OMVs, which benefit from a small size, adhesive properties, and ability to carry and deliver toxic components into host cells, have been proposed to play a significant role in the dissemination and delivery of virulence factors for Gram-negative pathogens (Ellis and Kuehn, 2010). The human pathogens *Vibrio cholerae*, *Vibrio vulnificus* and the fish pathogen *Vibrio anguillarum* are known to actively secrete OMVs during their growth (Chatterjee and Das, 1967; Hong *et al*., 2009; Kim *et al*., 2010). In several vibrio species, virulence factors have been proposed to be associated with such OMVs (Boardman *et al*., 2007; Kim *et al*., 2010). In addition, the release of OMVs by Gram-negative bacteria has recently been shown be protective against bacteriophages and antimicrobial peptides (AMPs) (Manning and Kuehn, 2011; Duperthuy *et al*., 2013). AMPs from both eukaryotic and prokaryotic origin have been evidenced in oyster haemolymph. Indeed, not only do haemocytes produce a broad series of endogenous AMPs (for review, Schmitt *et al*., 2012) but also bacteriocin-like peptides are present in oyster plasma (Defer *et al*., 2013). To date, little is known on the

effectors of AMP resistance in oyster pathogenic vibrios (Duperthuy *et al*., 2010) and the potential role of OMVs remains unexplored. While global proteomic studies of native OMVs are required to elucidate the functions of OMVs (Lee *et al*., 2008), global descriptions of OMV proteomes remain very scarce in *Vibrio* species.

Here we asked whether *V. tasmaniensis* LGP32 produces OMVs and how they are involved in pathogenesis by focusing on the delivery of virulence factors and the protection against AMPs. To this aim, we isolated OMVs from LGP32 ECPs, developed a global proteomic characterization of LGP32 OMVs and studied the interaction of OMVs with the oyster immune cells. Our results show that LGP32 secretes OMVs rich in hydrolases which can be internalized by host immune cells or be released by intraphagosomal bacteria. Among the encapsulated hydrolases, one major gelatinase/caseinase named Vsp (VS_II0815) for vesicular serine protease (Vsp) was found to be specifically secreted through OMV production. Vsp was shown here to participate in the virulence phenotype of LGP32 in oyster experimental infections. Besides, OMVs were shown to be protective against AMPs independently of Vsp activity.

Results

The strain LGP32 secretes OMVs

Vesicle production by LGP32 was first examined by electron microscopy. Logarithmic phase cultures of LGP32 showed the release of small vesicles with an average diameter of 30 to 50 nm, as revealed by negative staining. Vesicles were observed both in the culture medium and bound to the bacterial membrane and polar flagellum (Fig. 1A–E). ECPs were separated from *Vibrio* cells by centrifugation and filtration (0.2 µm). They were further ultracentrifuged to separate vesicles from soluble products. The isolated vesicles were intact and homogeneous as observed after negative staining by transmission electron microscopy (Fig. 1F). Their diameter ranged from 30 and 50 nm, consistent with the size observed before vesicle purification. The protein concentration of the vesicles released by LGP32 in Zobell medium was measured at 1 µg ml^{-1}.

The protein composition of the purified vesicles was determined by a proteomic approach consisting in stacking electrophoresis followed by trypsin digestion and peptide analysis using nanoliquid chromatography coupled to tandem mass spectrometry (nanoLC-MS/MS) sequencing. Two OMV preparations were analysed. The first preparation (OMV prep #1) corresponded to crude OMVs while the second preparation obtained independently (OMV prep #2) was further purified by density gradient. Protein identification was achieved using Mascot and sequences obtained from the LGP32 genome (Le Roux *et al*., 2009). Only proteins identified by more than three peptides were kept for further analysis. A total of 188 and 177 vesicle-associated proteins were identified in the OMV prep #1 and #2 respectively (Supporting Information Table S1). Only the 132 proteins common

to both preparations were considered to belong to the OMV proteome. A subcellular localization could be assigned to most of them (98.5%). Consistent with the composition expected for OMVs, Tat- and Sec-exported proteins, outer membrane and periplasmic proteins accounted for 88.6% of the identified proteins (Supporting Information Table S1). Most of the remaining proteins were identified as extracellular flagellar proteins (6.8%) (Supporting Information Table S2).

OMVs of LGP32 display a high content in proteases

Among the proteins identified, a large fraction (33 proteins, 25%) encoded enzymes such as proteases, sulfatases, phosphatases, nucleases and lipases (Supporting Information Table S1). We focused here on proteases, which can be important virulence factors in vibrios. Putative proteases are also the most abundant hydrolases found in our OMV proteomic analysis (15 proteins, 45.5% of the identified hydrolases, 11.4% of the identified proteins; Supporting Information Table S1). We asked whether such proteases were enclosed within OMVs. Intact OMVs (2 mg ml^{-1}) displayed little to no proteolytic activity when tested in the azocasein assay (Fig. 2A). This contrasted strongly with the soluble products of LGP32 ECPs (supernatant of ultracentrifuged ECPs), which displayed strong proteolytic activity at 1 mg ml^{-1} mainly due to the Vsm protease (Fig. 2A, Supporting Information Fig. S1). Interestingly, when OMVs were lysed by treatment with 0.1% Triton X-100
(Fig. 2C), major protease activity was detected (Fig. 2A), showing that proteases enclosed within OMVs were released upon membrane disruption.

A putative serine protease (VS_II0815) is the major gelatinase/caseinase of OMVs

To identify the OMV-associated protease(s), OMVs were subjected to zymography on both a casein- and a gelatincontaining polyacrylamide gel. On both substrates, one protease band was observed at an approximate molecular mass of 30 kDa (Fig. 2B). The same band was observed for OMVs from wild-type or Δ*vsm* LGP32 (Supporting Information Fig. S1) showing that this protease activity is not related to the *vsm* gene. Consistent with an intravesicular localization of the protease, no protease band at the same size was observed in supernatant depleted of OMVs (Supporting Information Fig. S1). The gelatinase activity was similar at 20°C and 37°C, and stable in a pH range of 5.6 to 7.7 (Supporting Information Fig. S2). The protease evidenced by zymography was identified by trypsin in-gel digestion followed by nanoLCMS/MS sequencing. A total of six peptides identified the protein (23% coverage), all of which aligned with the central-most region of the VS_II0815 sequence (Fig. 3), a putative S1 family-secreted trypsin-like serine protease (calculated mass 39 kDa). The vesicular serine protease (Vsp) isolated from OMVs was 47.5% identical to the VesA serine protease of V. cholerae VCA0803 (Fig. 3). To confirm that Vsp is the main gelatinase/caseinase observed on zymography of LGP32 OMVs, we constructed an isogenic deletion mutant. The LGP32 Δvsp mutant did not display any growth defect in Zobell growth medium nor in oyster plasma (Supporting Information Fig. S3A). We then compared the gelatin zymogram profile of OMVs obtained from the wild-type and Δvsp mutant. Upon vsp deletion, the active band assigned to Vsp disappeared from

the zymography (Fig. 2B). Altogether, our data show that Vsp (VS_II0815 gene product) is the major gelatinase/caseinase of LGP32 OMVs.

*The virulence of the Δ*vsp *mutant is attenuated in oyster experimental infections*

To determine whether Vsp could contribute to the virulence of LGP32, juvenile oysters were infected with the wild-type LGP32 or the Δvsp isogenic mutant. In two independent experiments, groups of 45 oysters received an injection of 4 × 107 colony-forming units (cfu) of each strain. No mortalities were recorded over 7 days for control oysters injected with sterile seawater (SSW). Interestingly, the Δvsp mutant was significantly impaired in terms of virulence compared with the wild-type LGP32 as revealed by Kaplan–Meier survival curves (P = 0.0004, log-rank test). Indeed, oyster mortalities at day 7 were reduced from 91.2% for the wild-type LGP32 to 55.7% for the Δvsp isogenic mutant (Fig. 4). Because in vivo complementation of the virulence phenotype could not be achieved due to the toxicity of the vsp gene product for the Escherichia coli donor strain, we tested two additional Δvsp mutants obtained independently in experimental infections. The Kaplan–Meier survival curves showed a significant attenuated phenotype for both mutants (P = 0.027 and P = 0.006) (Supporting Information Fig. S5). Consequently, it is very unlikely that the attenuated phenotype associated to the Δvsp deletion is due to a second site mutation. We concluded that the Δvsp deletion attenuates LGP32 virulence in oyster experimental infections.

OMVs can be delivered to host immune cells both intracellularly and extracellularly

The presence of Vsp inside OMVs prompted us to investigate the role of OMVs in the delivery of virulence factors to host cells in the course of LGP32 infectious process. We first asked whether OMVs could be secreted inside haemocytes during its intracellular stages. Haemocytes having phagocytosed LGP32 (30 min contact) were therefore observed by transmission electron microscopy. Vibrios were found inside phagosomes without any sign of bacterial cell envelope destruction nor lysis (Fig. 5A–D). When haemocytes contained only few vibrios, vibrios were observed as single cells inside phagosomes without evident haemocyte damage (Fig. 5A). When haemocytes were invaded by abundant vibrios (Fig. 5C and D), one to four vibrios were present inside large vacuoles and haemocytes displayed important cytoplasmic disorders with (i) a loss of integrity of intracellular organelles including endoplasmic reticulum and mitochondria, and (ii) an accumulation of vacuoles of heterogeneous sizes. No vibrios were observed in the cytoplasm of haemocytes outside phagosomes but some vacuoles containing vibrios displayed membrane disruptions. Damages to the haemocyte cytoplasmic membrane were also observed (Fig. 5D). Importantly, for the vast majority of infected haemocytes, vesicles of 30–50 nm diameter reminiscent of those observed in LGP32 culture medium were visible releasing from the bacterial membrane or free inside phagosomes (Fig. 5B and D). We then asked whether such OMVs, which

are also released extracellularly (Fig. 1), could enter host cells. For that, OMVs fluorescently labeled with PKH26 were incubated with haemocytes for 2 h. A strong red fluorescent signal was observed by confocal microscopy within haemocytes (Fig. 5E and F), indicating that OMVs were internalized upon contact with haemocytes.

OMVs confer protection against AMPs independently of Vsp

We then asked whether OMV production could confer protection against the AMPs found in oyster plasma. Indeed, a remarkable stimulation of OMV production was observed by electron microscopy when LGP32 was cultured in oyster plasma (Supporting Information Fig. S3C).

To test the protective effect of OMVs, LGP32 was exposed to a membrane-active AMP, polymyxin B (PmB) in the presence of OMVs isolated from the wild-type or the Δ*vsp* mutant. A dose-dependent protective effect of LGP32 OMVs was observed against PmB, whose minimal inhibitory concentration (MIC = 0.78 μM) increased by twofold in the presence of 6.25 μg ml^{-1} OMVs (protein concentration) and up to 16-fold in the presence of 50 μg ml^{-1} OMVs (Table 1). The same protection was obtained with 50 μg ml^{-1} OMVs from the Δ*vsp* mutant (Table 1). In addition, the MIC of PmB against the wild-type or the Δ*vsp* mutant were identical at 0.78 μM. Altogether, this indicates that OMVs provide a significant and dose-dependent protection against AMPs independently of *vsp* expression.

To determine whether the OMV-mediated protection could be conferred by enclosed proteases other than Vsp, we incubated PmB with wild-type OMVs for 6 h and monitored the PmB trace by reversed-phase high-performance liquid chromatography (RP-HPLC) and SDS-PAGE. No difference in the intensity of the PmB band was observed by SDS-PAGE, indicating that PmB is not degraded by intravesicular proteases (Fig. 6A). However, the highperformance liquid chromatography (HPLC) absorbance peak corresponding to PmB disappeared from the chromatogram over the time course of the incubation, indicating that at least PmB binds to OMVs (Fig. 6B). Altogether, our data indicate that PmB is not degraded but rather titrated by OMVs.

Discussion

Results showed that *V. tasmaniensis* strain LGP32 releases OMVs containing virulence factor(s) which can be delivered to host immune cells either intracellularly or extracellularly. A total of 132 proteins identified by at least three peptides were found associated to LGP32 OMVs (Supporting Information Table S1). In other bacterial species, 44 to 236 OMV-associated proteins were identified depending on the techniques used for proteomics (Lee *et al*., 2008). Most of the LGP32 OMV proteins were predicted to be Tat or Sec exported, to localize at the periplasm or at the outer membrane (88.6%) (Supporting Information Table S1). This composition is consistent with the biogenesis of Gram-negative OMVs (Deatherage *et al*., 2009; Kulp and Kuehn, 2010). Besides, 7.6%

of the proteins were predicted to be extracellular. Among them, 6.8% were flagellar proteins suggesting the presence of non-observed contaminating flagella. Surprisingly, flagellar proteins were still found when OMVs were purified by density gradient (Supporting Information Table S1). The observation of vesicles intimately associated with the flagellum by electron microscopy (Fig. 1C–E) suggests that OMVs can be released from the LGP32 flagella sheath
as also observed in *Vibrio fischeri* (Brennan *et al*., 2014). In *V. cholerae*, the flagella sheath was shown to be composed of the outer membrane, containing lipopolysaccharide (Fuerst and Perry, 1988) and outer membrane proteins (Bari *et al*., 2012). Interestingly, a recent study showed that OMVs from *E. coli* contain flagellar proteins (Manabe *et al*., 2013). It is therefore likely that the OMVs obtained from LGP32 contain both periplasmic and flagellar proteins as a result of different sites of biogenesis. Finally, 2.3% of the proteins were predicted to localize at the inner membrane. Such observations have also been made in other species, in which cytoplasmic and inner membrane potential virulence factors were found to be components of OMVs (for review, see Lee *et al*., 2008).

One major function characterizing the OMV proteome of LGP32 was enzymatic activities (25%). We indeed found several proteases, lipases, phospholipases, nucleases, haemolysins and murein hydrolases associated to OMVs, as revealed by MS-MS sequencing. Together with siderophore receptors and adhesins/ invasins, also found associated to LGP32 OMVs (Supporting Information Table S1), these hydrolases correspond to potential virulence factors described in pathogenic *Vibrio* species (Zhang and Austin, 2005; Méndez *et al*., 2012). Their association with OMVs is in agreement with the protease, phospholipase and haemolysin activities associated to OMVs of *V. anguillarum*, another pathogen for marine cultured species (Hong *et al*., 2009). Besides, consistent with the biogenesis and composition of OMVs, membrane transport (40.9%) and cell wall/membrane biogenesis (13.6%) were important functions associated to LGP32 OMV proteins. Indeed, we evidenced here many integral outer membrane proteins such as porins including the adhesin/invasin OmpU (Duperthuy *et al*., 2011), metal-siderophore transporters, ABC-transporters, efflux pumps and peptidoglycanassociated lipoproteins (Supporting Information Table S1). Altogether, molecular functions associated to LGP32 OMVs are similar to those found in OMVs from bacterial species other than vibrios (e.g. *E. coli*, *Neisseria meningitis*, *Pseudomonas antarctica*), which also display a large percentage of transport proteins (porins, ABC transporters), adhesins/invasins, but also hydrolases including potential virulence factors (proteases, haemolysins, murein hydrolases) and motility-related proteins (flagellins) (for review, see Lee *et al*., 2008).

One important finding from this study is that OMVs can be delivered to host cells both intracellularly, inside phagosomes and extracellularly, by internalization (Fig. 5). From our electron microscopy data, intracellular release of OMVs could be part of LGP32 infectious process. Indeed, we observed several vesicles attached to the bacteria as well as free vesicles of the same size (30–50 nm) inside the phagosome (Fig. 5B and D), which are likely released by the phagocytosed bacteria. Such vesicles were observed at early stages when few vibrios are present inside intact

haemocytes but also at late stages, when multiple vibrios are observed inside large vacuoles of damaged haemocytes (Fig. 5A–D). The absence of cytosolic vibrios in invaded haemocytes clearly showed that LGP32 behaves as an intravacuolar pathogen. Interestingly, in *Legionella pneumophila*, a facultative intracellular pathogen replicating inside vacuoles of macrophages, intracellular release of OMVs was also observed, OMVs being found to inhibit the fusion of phagosomes with lysosomes (Fernandez-Moreira *et al*., 2006). Since we earlier showed that LGP32 inhibits phagosome maturation (Duperthuy *et al*., 2011), one can hypothesize that, as in *L. pneumophila*, OMV release participates in the intracellular survival of LGP32. It can also be hypothesized that OMVs of LGP32 are vehicles for the delivery of candidate virulence factors to oyster immune cells (Fig. 5). Indeed, the OMV-mediated extracellular delivery of virulence factors to host cells has been reported in *Aggregatibacter actinomycetemcomitans* and *V. cholerae* (Chatterjee and Chaudhuri, 2011; Rompikuntal *et al*., 2012).

By focusing on proteases, we showed that potential virulence factors are specifically enclosed within OMVs. Indeed, while low proteolytic activity was associated to intact OMVs, major activity was released upon Triton lysis of OMVs (Fig. 2A). The gelatinase/caseinase activity enclosed in LGP32 OMVs was attributed to the putative serine protease VS_II0815, as revealed by MS-MS sequencing of the active band (Fig. 3) and zymography of a Δ*vsp* deletion mutant (Fig. 2B). Importantly, VS_II0815 was absent from the soluble fraction of LGP32 ECPs, i.e. ultracentrifuged supernatant devoid of OMVs (Supporting Information Fig. S1), showing it is specifically secreted through OMV release. VS_II0815 was therefore termed Vsp for vesicular serine protease. To our knowledge, such a specific intravesicular secretion of proteases is shown here for the first time. These observations are consistent with the view that OMVs can be considered as a secretion system *per se* (Lee *et al*., 2008). Noteworthy, we also showed that the previously characterized Vsm (Le Roux *et al*., 2007) was extravesicular, its gelatinase/caseinase activity being dominant in the supernatants after ultracentrifugation of ECPs but absent in OMVs (Supporting Information Fig. S1). Therefore, its identification by MS-MS sequencing (Supporting Information Table S1), which is a very sensitive technique, was attributed to its high abundance in the extracellular milieu, contaminating our OMV preparation.

The OMV-secreted Vsp protease was shown to be homologous to the VesA serine protease of *V. cholerae* (Sikora *et al*., 2011) (47.5% sequence identity). Like VesA, it carries the canonical catalytic triad His95Asp149-Ser254 as well as three out of the four conserved disulfide bridges of serine proteases (Fig. 3). In addition to a 29 residue signal peptide at N-terminal position, Vsp displays a potential transmembrane domain at its C-terminus. Both features are conserved in VesA (Fig. 3). This C-terminal transmembrane domain can either be a sorting signal or an inner membrane anchor. The lack of peptides identified by MS-MS at the N- and C-terminus of the Vsp protease as well as its apparent mass on a polyacrylamide gel electrophoresis (30 kDa), lower than its calculated mass (39 kDa), strongly suggest that the Vsp protein isolated from OMVs results from the posttranslational

maturation of a larger precursor. Taken together with its localization inside OMVs, this indicates that Vsp is likely addressed to the inner membrane through its signal peptide, retained at the inner membrane by its Gly335-Phe353 C-terminal inner membrane anchor and finally released into the periplasmic space upon proteolytic maturation. Such maturation could occur at several sites between residues 280 and 335, in the region separating the serine protease domain of Vsp from its C-terminal anchor. Indeed two Arg residues recognized by trypsin-like serine proteases as well as a Lys-Arg and a Arg–Arg–Arg multibasic site recognized by kexin-like serine proteases (Kobayashi *et al*., 2009) are found in this region (Fig. 3). In *V. cholera*e, VesA was proposed to be transported through the type II secretion system (T2SS) but could not be observed in ultracentrifuged culture supernatants (Sikora *et al*., 2011). Because VesA lacks the Lys-Arg and Arg–Arg–Arg multibasic sites found in the Vsp sequence (Fig. 3), it could be retained at the inner membrane of *V. cholerae*.

Importantly, the virulence of three Δ*vsp* mutants was shown to be attenuated compared with the wild-type LGP32 in oyster experimental infections (Fig. 4 and Supporting Information Fig. S5). Therefore, we concluded that like other proteases involved in host–*Vibrio* pathogenic interactions (Shinoda and Miyoshi, 2011), the serine protease Vsp participates in the virulence phenotype of LGP32. This demonstrates that the OMV-mediated delivery of virulence factors contributes to LGP32 pathogenesis. Remarkably, unlike Vsp, the major metalloprotease Vsm, which was shown here to be extravesicular (Supporting Information Fig. S1), did not significantly modify the virulence status of LGP32 in experimental infections (Le Roux *et al*., 2007). It is still unknown at what stage of the pathogenesis Vsp is involved. Indeed, the Δ*vsp* deletion mutants did not show any evident phenotype on haemocyte primary cultures (data not shown), suggesting that Vsp does not have a direct effect on oyster haemocytes. Thus, the major phenotype observed in oyster experimental infections could rely on Vspdependent virulence factors expressed *in vivo*. For instance, Vsp could be required for the proteolytic activation of LGP32 virulence factors as demonstrated for its homologue VesA from *V. cholerae*, which activates the CtxA cholera toxin by proteolytic cleavage (Sikora *et al*., 2011).

Besides Vsp, potential virulence factors associated to OMVs of LGP32 deserve further investigation to better understand the role of OMVs in pathogenesis. Two putative haemolysins and a phospholipase D (PLD) found in our proteomic data (Supporting Information Table S1) are of particular interest. These toxins are indeed known for their lytic properties on biological membranes, causing damage to erythrocytes and other cell types, such as leukocytes or neutrophils (for review, see Méndez *et al*., 2012). PLD are involved in virulence of different bacteria. In the intracellular pathogen *Corynebacterium pseudotuberculosis*, secreted PLD can be lethal for neutrophils and macrophages in which it is expressed at high levels (Yozwiak and Songer, 1993; McKean *et al*., 2007). Haemolysins are the most widely distributed toxins among pathogenic vibrios (Zhang and Austin, 2005). In *V. vulnificus*, expression of the cytolysin-haemolysin VvhA in response to low-iron concentrations results in erythrocytes lysis providing iron for bacterial growth and

pathogenicity (Lee *et al*., 2013). VvhA was shown to be delivered to mouse cells through OMV secretion (Kim *et al*., 2010). Therefore, it is tempting to speculate that secretion of cytolytic enzymes such as haemolysins and PLD through OMV release (Fig. 5B and D) participates in the disruption of vacuole and cytoplasmic membrane observed when high numbers of intracellular vibrios are present inside haemocytes (Fig. 5D). Future functional studies will help identifying how far such OMV-associated proteins participate in the virulence phenotype of LGP32. Finally, OMVs from LGP32 were shown here to be highly protective against AMPs, increasing the MIC of PmB from 2- to 16-fold at OMV concentrations ranging from 6.25 to 50 μg ml^{-1} (Table 1). We believe that such OMV concentrations can be reached in oyster plasma. Indeed, while OMV production was rather low in rich culture medium (1 μg ml^{-1}), it increased strongly in the presence of plasma (Supporting Information Fig. S3). The role of proteases in resistance to AMPs has been shown in several bacterial species (Nizet, 2006). However, OMV protection against AMPs was not conferred by Vsp since (i) sensitivity to PmB was similar for the wild-type and Δ*vsp* mutant (Table 1), (ii) OMVs from the wild-type and Δ*vsp* mutant were similarly protective against PmB (Table 1), and (iii) PmB was not degraded upon contact with OMVs (Fig. 6). Rather, we found that OMV protection relies on titration by OMVs, probably due to the membrane insertion properties of PmB into biological membranes (Tomarelli *et al*., 1949). Recent data on *V. cholerae* showed that only OMVs carrying the biofilmassociated extracellular matrix protein Bap1 were protective against the human AMP LL-37, with an increase of MIC by fourfold (Duperthuy *et al*., 2013). As in LGP32, protection resulted from trapping of LL-37 and did not require proteolytic degradation of LL-37. Therefore, while the molecular bases of AMP binding to OMVs appear to differ among *Vibrio* species, OMVs similarly protect vibrios from AMPs by forming a protective shield in which AMPs are entrapped. A similar protective role was also recently proposed for *E. coli* OMVs on which both bacteriocins (AMPs from prokaryotic origin) and bacteriophages were found to be adsorbed, thus contributing to bacterial defences (Manning and Kuehn, 2011). Since AMPs are both produced by the oyster microbiota and oyster tissues (Schmitt *et al*., 2012; Defer *et al*., 2013), OMV production may confer a major advantage for vibrios to colonize oysters.

Experimental procedures

Bacterial strains and culture condition

Escherichia coli strains Π3813 and β3914 (Le Roux *et al*., 2007) were used for cloning and conjugation respectively. *Escherichia coli* strains were grown in Luria–Bertani (LB) at 37°C (Difco). The *Vibrio* strains (Supporting Information Table S3) were grown at 20°C either in artificial seawater (0.6 M NaCl, 20 mM KCl, 5 mM MgSO4, 1.4 mM MgCl2) supplemented with 4 g l^{-1} bactopeptone and 1 g l^{-1} yeast extract (referred to as Zobell medium) or in LB supplemented with NaCl 0.5 M (LB-NaCl). Chloramphenicol was used at 12.5 μg ml^{-1}. Thymidine and diaminopimelate were supplemented when necessary to a final concentration of 0.3 mM. Induction of *ccdB* expression under the control

of P_{BAD} promoter was achieved by the addition of 0.2% L-arabinose to the growth media and repressed by 1% D-glucose.

Vector construction and mutagenesis

The LGP32 Δ*vsp* derivative was constructed by allelic exchange using the method described previously (Le Roux *et al*., 2007). Briefly, alleles carrying an internal deletion were generated *in vitro* using a two-step polymerase chain reaction (PCR) construction method (Binesse *et al*., 2008) using primers 281112-1 to 4 (Supporting Information Table S3) and cloned into PSW7848T, a R6K γ-*ori*-based suicide vector that encodes the *ccdB* toxin gene under the control of an arabinose-inducible and glucose-repressible promoter, P_{BAD}. Matings between *E. coli* and *Vibrio* were performed at 30°C as described previously (Le Roux *et al*., 2007). Selection of the plasmid-borne drug marker resulted in integration of the entire plasmid in the chromosome by a single crossover. Elimination of the plasmid backbone resulting from a second recombination step was selected by arabinose induction of the *ccdB* toxin gene. Mutants were screened by PCR using primers 281112-1 and 4. *vsp* deletion was verified by sequencing using primers VS_II0815-Fw2 and VS_II0815Rv2 (Supporting Information Table S3).

ECPs and OMV preparation

Bacterial ECP were produced by the cellophane overlay method described by Liu (1957). Briefly, 2 ml of stationary phase culture were spread onto a Zobell agar plate covered by a sterile cellophane film. After 48 h of incubation at 20°C, the cellophane overlay was transferred to an empty Petri dish. Cells were harvested in 250 µl of 0.1 M cold sodiumphosphate buffer (pH 7). Bacterial cells were removed by centrifugation at 16 000 *g* at 4°C for 30 min. The supernatant was filtered through a 0.22 µm-pore-size polyvinylidene difluoride (PVDF) membrane filter (Millipore). OMVs were obtained from ECPs by ultracentrifugation at 100 000 *g* for 2 h at 4°C using a TLA110 rotor (Beckman Instruments). The ultracentrifuged supernatant (Sn) was kept at −20°C while crude OMVs were washed with 0.1 M cold sodium-phosphate buffer (pH7) and suspended in cold phosphate-buffered saline (PBS) (Wai *et al*., 2003). When OMVs were purified by density gradient centrifugation, Optiprep gradient was used as described previously (Balsalobre *et al*., 2006). Briefly, crude OMVs preparations suspended in PBS buffer were added on the top of gradient layers and centrifuged at 100 000 *g* for 3 h at 4°C. Fractions of 200 µl were sequentially collected from the top of the ultracentrifugation tube and analysed by SDS-PAGE and immunoblotting using antiOmpU antiserum to identify the fractions containing OMVs. The OMVs protein concentration was determined by the Bradford method with Micro-BCA protein assay reagent (Pierce Biotechnology, Rockford, IL, USA). OMVs were stored at −20°C until use.

Protease activity quantification

Protease activity of ECPs, intact or lysed OMVs, was determined using azocasein (Sigma A2765) as a substrate. When indicated, OMVs 2 mg ml^{-1} were lysed for 30 min at 20°C in PBS containing 0.1% Triton X-100 (Sigma T8787). Intact OMVs were kept in PBS. Then, 100 µl of azocasein (5 mg ml^{-1} in 100 mM Tris-HCl buffer, pH 8.5) were added to 50 µl of OMVs preparations. The mixture was incubated at 20°C for 1 h. The undigested substrate was precipitated by adding 100 µl of 10% trichloroacetic acid to the reaction mixture during 5 min on ice, followed by centrifugation at 12 000 *g* and 4°C for 5 min. The supernatant (100 µl) was neutralized by addition of an equal volume of 1 N NaOH. After mixing, the absorbance at 440 nm was determined
(Tomarelli *et al*., 1949). Significance of differences was determined using a Student's *t*-test.

Gelatin zymography

OMVs were analysed for protease activity by a gelatin substrate gel electrophoresis. Five microgram of OMVs resuspended in loading buffer [62.5 mM Tris HCl, pH 6.8, 4% SDS (w/v), 20% (v/v) glycerol and 0.001% bromophenol blue] in the absence of reducing agents were loaded onto a 12.5% SDS-PAGE containing 0.2% gelatin. After electrophoresis, the gels were washed in renaturing buffer (50 mM Tris-HCl pH 7.6 and 2.5% Triton X-100) for 2 h at room temperature, and then incubated overnight at 37°C in the developing buffer (50 mM Tris-HCl pH 7.6, 200 mM NaCl, 5 mM $CaCl_2$, 0.02% w/v Brij 35). The gels were stained with a solution containing 0.1% Coomassie brilliant blue R-250. Formation of clear zone against the blue background on the polyacrylamide gels indicated the gelatinolytic activity (Binesse *et al*., 2008).

Proteomic and LC-MS/MS analyses

Protein preparation and digestion. OMV proteins solubilized in Laemmli buffer were stacked in the top of a 4–12% NuPAGE gel (Invitrogen) before R-250 Coomassie blue staining. The gel band was manually excised and cut in pieces before being washed by six successive incubations of 15 min in 25 mM NH_4HCO_3 and in 25 mM NH_4HCO_3 containing 50%
(v/v) acetonitrile. Gel pieces were then dehydrated with 100% acetonitrile and incubated for 45 min at 53°C with 10 mM Dithiothreitol (DTT) in 25 mM NH_4HCO_3 and for 35 min in the dark with 55 mM iodoacetamide in 25 mM NH_4HCO_3. Alkylation was stopped by adding 10 mM DTT in 25 mM NH_4HCO_3 and mixing for 10 min. Gel pieces were then washed again by incubation in 25 mM NH_4HCO_3 before dehydration with 100% acetonitrile. Modified trypsin (Promega, sequencing grade) in 25 mM NH_4HCO_3 was added to the dehydrated gel pieces for an overnight incubation at 37°C. Peptides were then extracted from gel pieces in three 15 min sequential extraction steps in 30 µl of 50% acetonitrile, 30 µl of 5% formic acid and finally 30 µl of 100% acetonitrile. The pooled supernatants were then dried under vacuum.

Nano-LC-MS/MS analyses. The dried extracted peptides were resuspended in 5% acetonitrile and 0.1% trifluoroacetic acid (TFA) and analysed by online nanoLC-MS/MS (Ultimate 3000, Dionex and LTQ-Orbitrap Velos pro, Thermo Fischer Scientific). Peptides were sampled on a 300 µm × 5 mm PepMap C18 precolumn and separated on a 75 µm × 250 mm C18 column (PepMap, Dionex). The nanoLC method consisted in a 120 min gradient at a flow rate of 300 nl min^{-1}, ranging from 5% to 37% acetonitrile in 0.1% formic acid during 114 min before reaching 72% acetonitrile in 0.1% formic acid for the last 6 min. Mass spectrometry (MS) and MS/MS data were acquired using Xcalibur (Thermo Fischer Scientific). Spray voltage and heated capillary were respectively set at 1.4 kV and 200°C. Survey full-scan MS spectra (m/z = 400–1600) were acquired in the Orbitrap with a resolution of 60 000 after accumulation of 106 ions (maximum filling time: 500 ms). The 20 most intense ions from the preview survey scan delivered by the Orbitrap were fragmented by collision-induced dissociation (collision energy 35%) in the LTQ after accumulation of 104 ions (maximum filling time: 100 ms).

Bioinformatics analyses. Data were processed automatically using Mascot Daemon software (version 2.3.2, Matrix Science). Concomitant searches against LGP32 and classical contaminant protein sequence databases (4500 sequences) and the corresponding reversed databases were performed using Mascot (version 2.4). ESI-TRAP was chosen as the instrument, trypsin/P as the enzyme and two missed cleavage allowed. Precursor and fragment mass error tolerances were set respectively at 10 ppm and 0.6 Da. Peptide modifications allowed during the search were: carbamidomethyl (C, fixes) acetyl (N-ter, variable), oxidation (M, variable) and deamidation (NQ, variable). The IRMa software (Dupierris *et al*., 2009) was used to filter the results: conservation of rank 1 peptides, peptide identification False Discovery Rate (FDR) < 1% (as calculated on peptide scores by employing the reverse database strategy) and minimum of three specific peptide per identified protein group.

Sequence annotation and subcellular localization

Functional annotation of coding DNA sequences was manually assigned based on automated annotation generated by the MicroScope platform pipeline (Vallenet *et al*., 2013) combined with BlastP analysis, PFAM (Punta *et al*., 2012) and InterProScan search (Quevillon *et al*., 2005). Protein subcellular localization (SCL) were predicted using a consensus-based approach that combine SCL tools results grouped by predicted features: Sec-dependent signal peptides was predicted using SignalP v4.0 (Petersen *et al*., 2011), PrediSi (Hiller *et al*., 2004) and Phobius v1.01 (Kall *et al*., 2004); twin-arginine (TAT) signal peptides using TatFind Server (Rose *et al*., 2002); lipoprotein signal peptides and membrane retention signal using LIPO (Berven *et al*., 2006), LipoP v1.0 (Rahman *et al*., 2008) and PRED-LIPO (Bagos *et al*., 2008); transmembrane α-helix (except signal peptide) of inner membrane protein using TMHMM v2.0 (Krogh *et al*., 2001), HMMTOP v2.0 (Tusnady and Simon, 2001) and Phobius v1.01; outer membrane protein using HHomp (Remmert *et al*., 2009); and global

prediction using PSORTb v3.0.2 (Yu *et al*., 2010), CELLO v2.5 (Yu *et al*., 2006) and SOSUIGramN (Imai *et al*., 2008). Enzymes were identified using the MEROPS database (Rawlings *et al*., 2012).

Experimental infection of oysters

Juvenile and adult diploid *C. gigas* were purchased from the Ifremer oyster hatchery in La Tremblade (Charente Maritime, France) and from a local oyster farm in Mèze (Gulf of Lion, France) respectively. Experimental infections were performed at 20°C, as previously described (Duperthuy *et al*., 2010). Groups of 45 oysters were injected with wild-type or Δ*vsp* LGP32 (4×10^7 cfu per juvenile oyster or 2×10^8 cfu per adult oyster). Control animals were injected with an equal volume of SSW. For every condition, oysters were placed for 24 h in three separate tanks in 10 l of seawater (15 animals per tank). Mortalities were monitored daily over 7 days. The nonparametric Kaplan–Meier test was used to estimate log-rank values for comparing the survival curves (Kaplan and Meier, 1958). All experimental infections were performed according to the Ifremer animal care guideline and policy.

Observation of extracellular and intracellular OMVs by electron microscopy

For extracellular OMVs, logarithmic phase culture of LGP32 were negatively stained with 0.1% uranyl acetate and then placed on carbon-coated Formvar grids. To visualize intracellular OMVs, haemolymph was first collected from the pericardial cavity of oysters using a 2 ml syringe equipped with a 23-G needle. After counting, haemocytes were infected at a multiplicity of infection of 50:1 (30 min, room temperature) with stationary phase LGP32 previously opsonized with oyster plasma as described earlier (Duperthuy *et al*., 2011). After extensive washing, the cells were fixed with sterile seawater containing 2.5% glutaraldehyde for 1 h. Postfixation was achieved in 1% osmium tetroxide for 1 h at room temperature in the dark. Excess fixing agents were eliminated during dehydration of samples in a graded series of aqueous solution containing increasing amounts of ethanol finishing by absolute acetone. Finally, dehydrated samples were embedded in epoxy resin (EmBed 812). Sections (70 nm thick) were stained with uranyl acetate. All preparations were examined under a Hitachi 7100 transmission electron microscope at the 'Centre de Ressources en Imagerie Cellulaire' platform of Montpellier, France.

Uptake of PKH26-labeled OMVs by oyster haemocytes

OMVs (2 mg ml^{-1}) were labeled with 10^{-6} M PKH26 red fluorescent dye (MINI26-Sigma) as described previously (Duperthuy *et al*., 2013). After two washes in PBS followed by a 1 h-centrifugation at 100 000 *g*, the PKH26-labeled OMVs were resuspended in PBS. Monolayers of 5×10^5 haemocytes obtained by dispensing freshly collected haemolymph on glass coverslips in a 24-well plate (Costar 3526) were exposed for 2 h to PKH26-labeled OMVs (60 µg per well). After fixation with 4% paraformaldehyde in SSW, haemocytes were washed twice with PBS and stained with 0.5 µg ml^{-1} Phalloidin Alexa488 (Invitrogen) and 0.25 µg ml^{-1} 4,6-diamidino-2-phenylindole (Sigma).

Photographs were acquired on a Leica SPE confocal laser scanning system connected to a Leica DM2500 upright microscope.

Antimicrobial assays

Serial dilutions of OMVs (6.25–50 μg ml^{-1}) were co-incubated with different concentrations of PmB (Fluka P9602) for 1 h at 20°C prior to liquid growth inhibition assay using LGP32. Liquid growth inhibition assays were performed in microtiter plates as described in Hetru and Bulet (1997) using exponential phase cultures of LGP32 diluted in fresh in Zobell medium at a theorical starting OD_{600} of 0.001. Incubation was performed for 16 h at 20°C and bacterial density was determined spectrophotometrically at 600 nm by using a Multiscan microplate reader (LabSystem). The MIC was determined as the lower PmB concentration inhibiting 100% growth.

HPLC and SDS-PAGE monitoring of PmB

PmB (30 μg) was co-incubated with OMVs (100 μg) or sterile water for 4 h and 6 h at 20°C. Samples (50 μl) were analysed by C18 RP-HPLC column (UP5ODB 25QS, 120 Å, 5 μm, 250 × 2.0 mm, Interchim) using a linear 0–70% gradient of acetonitrile in 0.05% trifluoroacetic acid (TFA) over 35 min at a flow rate of 0.7 ml min^{-1}. In parallel, PmB (0.6 μg) was co-incubated with OMVs (2 μg) or sterile water for 4 h at 20°C. Samples were separated on a 12.5% Tris-glycine sodium dodecyl sulfate-polyacrylamide gel and stained with silver nitrate.

Acknowledgements

We are grateful to Agnès Vergnes, Julie Nicod and Marc Leroy for technical assistance. We are indebted to Chantal Cazevieille (Centre de Ressources en Imagerie Cellulaire de Montpellier, France) for precious expertise in electron microscopy, as well as to the Montpellier RIO Imaging platform of University of Montpellier 2 for access to confocal microscopy. We also thank Dr Alain Givaudan, Dr Michel Vidal, Dr Evelyne Bachère, Dr Julien de Lorgeril and Professor Estelle JumasBilak at the University of Montpellier for fruitful discussions. This work received financial support from the ANR (Vibriogen project, Blanc SVSE7 2011). A.S.V. received fellowship from the Ifremer and the University of Montpellier 1 (graduate student grant).

References

Bagos, P.G., Tsirigos, K.D., Liakopoulos, T.D., and Hamodrakas, S.J. (2008) Prediction of lipoprotein signal peptides in Gram-positive bacteria with a hidden Markov model. *J Proteome Res* **7:** 5082–5093.

Balsalobre, C., Silvan, J.M., Berglund, S., Mizunoe, Y., Uhlin, B.E., and Wai, S.N. (2006) Release of the type I secreted alpha-haemolysin via outer membrane vesicles from *Escherichia coli*. *Mol Microbiol* **59:** 99–112.

Bari, W., Lee, K.M., and Yoon, S.S. (2012) Structural and functional importance of outer membrane proteins in *Vibrio cholerae* flagellum. *J Microbiol* **50:** 631–637.

Berven, F.S., Karlsen, O.A., Straume, A.H., Flikka, K., Murrell, J.C., Fjellbirkeland, A., *et al*. (2006) Analysing the outer membrane subproteome of *Methylococcus capsulatus* (Bath) using proteomics and novel biocomputing tools. *Arch Microbiol* **184:** 362–377.

Beveridge, T.J. (1999) Structures of gram-negative cell walls and their derived membrane vesicles. *J Bacteriol* **181:** 4725–4733.

Binesse, J., Delsert, C., Saulnier, D., Champomier-Verges, M.C., Zagorec, M., Munier-Lehmann, H., *et al*. (2008) Metalloprotease Vsm is the major determinant of toxicity for extracellular products of *Vibrio splendidus*. *Appl Environ Microbiol* **74:** 7108–7117.

Boardman, B.K., Meehan, B.M., and Fullner Satchell, K.J. (2007) Growth phase regulation of *Vibrio cholerae* RTX toxin export. *J Bacteriol* **189:** 1827–1835.

Brennan, C.A., Hunt, J.R., Kremer, N., Krasity, B.C., Apicella, M.A., McFall-Ngai, M.J., and Ruby, E.G. (2014) A model symbiosis reveals a role for sheathed-flagellum rotation in the release of immunogenic lipopolysaccharide. *Elife* **3:** e01579.

Chatterjee, D., and Chaudhuri, K. (2011) Association of cholera toxin with *Vibrio cholerae* outer membrane vesicles which are internalized by human intestinal epithelial cells. *FEBS Lett* **585:** 1357–1362.

Chatterjee, S.N., and Das, J. (1967) Electron microscopic observations on the excretion of cell-wall material by *Vibrio cholerae*. *J Gen Microbiol* **49:** 1–11.

Deatherage, B.L., Lara, J.C., Bergsbaken, T., Rassoulian Barrett, S.L., Lara, S., and Cookson, B.T. (2009) Biogenesis of bacterial membrane vesicles. *Mol Microbiol* **72:** 1395–1407.

Defer, D., Desriac, F., Henry, J., Bourgougnon, N., Baudy-Floc'h, M., Brillet, B., *et al*. (2013) Antimicrobial peptides in oyster hemolymph: the bacterial connection. *Fish Shellfish Immunol* **34:** 1439–1447.

Duperthuy, M., Binesse, J., Le Roux, F., Romestand, B., Caro, A., Got, P., *et al*. (2010) The major outer membrane protein OmpU of *Vibrio splendidus* contributes to host antimicrobial peptide resistance and is required for virulence in the oyster *Crassostrea gigas*. *Environ Microbiol* **12:** 951– 963.

Duperthuy, M., Schmitt, P., Garzón, E., Caro, A., Rosa, R.D., Le Roux, F., *et al*. (2011) Use of OmpU porins for attachment and invasion of *Crassostrea gigas* immune cells by the oyster pathogen *Vibrio splendidus*. *Proc Natl Acad Sci USA* **108:** 2993–2998.

Duperthuy, M., Sjostrom, A.E., Sabharwal, D., Damghani, F., Uhlin, B.E., and Wai, S.N. (2013) Role of the *Vibrio cholerae* matrix protein Bap1 in cross-resistance to antimicrobial peptides. *PLoS Pathog* **9:** e1003620.

Dupierris, V., Masselon, C., Court, M., Kieffer-Jaquinod, S., and Bruley, C. (2009) A toolbox for validation of mass spectrometry peptides identification and generation of database: IRMa. *Bioinformatics* **25:** 1980–1981.

Ellis, T.N., and Kuehn, M.J. (2010) Virulence and immunomodulatory roles of bacterial outer membrane vesicles. *Microbiol Mol Biol Rev* **74:** 81–94.

Fernandez-Moreira, E., Helbig, J.H., and Swanson, M.S. (2006) Membrane vesicles shed by *Legionella pneumophila* inhibit fusion of phagosomes with lysosomes. *Infect Immun* **74:** 3285–3295.

Fuerst, J.A., and Perry, J.W. (1988) Demonstration of lipopolysaccharide on sheathed flagella of *Vibrio cholerae* O:1 by protein A-gold immunoelectron microscopy. *J Bacteriol* **170:** 1488–1494.

Gay, M., Renault, T., Pons, A.M., and Le Roux, F. (2004) Two *vibrio splendidus* related strains collaborate to kill *Crassostrea gigas*: taxonomy and host alterations. *Dis Aquat Organ* **62:** 65–74.

Hetru, C., and Bulet, P. (1997) Strategies for the isolation and characterization of antimicrobial peptides of invertebrates. *Methods Mol Biol* **78:** 35–49.

Hiller, K., Grote, A., Scheer, M., Munch, R., and Jahn, D. (2004) PrediSi: prediction of signal peptides and their cleavage positions. *Nucleic Acids Res* **32:** W375–W379.

Hong, G.E., Kim, D.G., Park, E.M., Nam, B.H., Kim, Y.O., and Kong, I.S. (2009) Identification of *Vibrio anguillarum* outer membrane vesicles related to immunostimulation in the Japanese flounder, *Paralichthys olivaceus*. *Biosci Biotechnol Biochem* **73:** 437–439.

Imai, K., Asakawa, N., Tsuji, T., Akazawa, F., Ino, A., Sonoyama, M., and Mitaku, S. (2008) SOSUI-GramN: high performance prediction for sub-cellular localization of proteins in gram-negative bacteria. *Bioinformation* **2:** 417– 421.

Kall, L., Krogh, A., and Sonnhammer, E.L. (2004) A combined transmembrane topology and signal peptide prediction method. *J Mol Biol* **338:** 1027–1036.

Kaplan, E.L., and Meier, P. (1958) Non parametric estimation for incomplete observations. *J Am Stat Assoc* **53:** 457– 481.

Kim, Y.R., Kim, B.U., Kim, S.Y., Kim, C.M., Na, H.S., Koh, J.T., *et al*. (2010) Outer membrane vesicles of *Vibrio vulnificus* deliver cytolysin-hemolysin VvhA into epithelial cells to induce cytotoxicity. *Biochem Biophys Res Commun* **399:** 607–612.

Kobayashi, H., Utsunomiya, H., Yamanaka, H., Sei, Y., Katunuma, N., Okamoto, K., and Tsuge, H. (2009) Structural basis for the kexin-like serine protease from *Aeromonas sobria* as sepsis-causing factor. *J Biol Chem* **284:** 27655–27663.

Kremer, N., Philipp, E.E., Carpentier, M.C., Brennan, C.A., Kraemer, L., Altura, M.A., *et al*. (2013) Initial symbiont contact orchestrates host-organ-wide transcriptional changes that prime tissue colonization. *Cell Host Microbe* **14:** 183–194.

Krogh, A., Larsson, B., von Heijne, G., and Sonnhammer, E.L. (2001) Predicting transmembrane protein topology with a hidden Markov model: application to complete genomes. *J Mol Biol* **305:** 567–580.

Kuehn, M.J., and Kesty, N.C. (2005) Bacterial outer membrane vesicles and the host-pathogen interaction. *Genes Dev* **19:** 2645–2655.

Kulp, A., and Kuehn, M.J. (2010) Biological functions and biogenesis of secreted bacterial outer membrane vesicles. *Annu Rev Microbiol* **64:** 163–184.

Labreuche, Y., Soudant, P., Goncalves, M., Lambert, C., and Nicolas, J.L. (2006) Effects of extracellular products from the pathogenic *Vibrio aestuarianus* strain 01/32 on lethality and cellular immune responses of the oyster *Crassostrea gigas*. *Dev Comp Immunol* **30:** 367–379.

Labreuche, Y., Le Roux, F., Henry, J., Zatylny, C., Huvet, A., Lambert, C., *et al*. (2010) *Vibrio aestuarianus* zinc metalloprotease causes lethality in the Pacific oyster *Crassostrea gigas* and impairs the host cellular immune defenses. *Fish Shellfish Immunol* **29:** 753–758.

Le Roux, F., Binesse, J., Saulnier, D., and Mazel, D. (2007) Construction of a *Vibrio splendidus* mutant lacking the metalloprotease gene *vsm* by use of a novel counterselectable suicide vector. *Appl Environ Microbiol* **73:** 777–784.

Le Roux, F., Zouine, M., Chakroun, N., Binesse, J., Saulnier, D., Bouchier, C., *et al*. (2009) Genome sequence of *Vibrio splendidus*: an abundant planctonic marine species with a large genotypic diversity. *Environ Microbiol* **11:** 1959– 1970.

Lee, E.Y., Choi, D.S., Kim, K.P., and Gho, Y.S. (2008) Proteomics in gram-negative bacterial outer membrane vesicles. *Mass Spectrom Rev* **27:** 535–555.

Lee, H.J., Kim, J.A., Lee, M.A., Park, S.J., and Lee, K.H. (2013) Regulation of haemolysin (VvhA) production by ferric uptake regulator (Fur) in *Vibrio vulnificus*: repression of *vvhA* transcription by Fur and proteolysis of VvhA by Fur-repressive exoproteases. *Mol Microbiol* **88:** 813– 826.

Lindell, K., Fahlgren, A., Hjerde, E., Willassen, N.P., Fallman, M., and Milton, D.L. (2012) Lipopolysaccharide O-antigen prevents phagocytosis of *Vibrio anguillarum* by rainbow trout (*Oncorhynchus mykiss*) skin epithelial cells. *PLoS ONE* **7:** e37678.

Liu, P.V. (1957) Survey of hemolysin production among species of pseudomonads. *J Bacteriol* **74:** 718–727.

McKean, S.C., Davies, J.K., and Moore, R.J. (2007) Expression of phospholipase D, the major virulence factor of *Corynebacterium pseudotuberculosis*, is regulated by multiple environmental factors and plays a role in macrophage death. *Microbiology* **153:** 2203–2211.

Manabe, T., Kato, M., Ueno, T., and Kawasaki, K. (2013) Flagella proteins contribute to the production of outer membrane vesicles from *Escherichia coli* W3110. *Biochem Biophys Res Commun* **441:** 151–156.

Manning, A.J., and Kuehn, M.J. (2011) Contribution of bacterial outer membrane vesicles to innate bacterial defense. *BMC Microbiol* **11:** 258.

Manning, A.J., and Kuehn, M.J. (2013) Functional advantages conferred by extracellular prokaryotic membrane vesicles. *J Mol Microbiol Biotechnol* **23:** 131–141.

Méndez, J., Reimundo, P., Pérez-Pascual, D., Navais, R., Gómez, E., Cascales, D., and Guijarro, J.A. (2012) An overview of virulence-associated factors of Gram-negative fish pathogenic bacteria. In *Health and Environment in Aquaculture*. Carvalho, D.E. (ed.). Rijeka, Croatia: InTech, pp. 133–156.

Miyoshi, S., and Shinoda, S. (2000) Microbial metalloproteases and pathogenesis. *Microbes Infect* **2:** 91–98.

Nizet, V. (2006) Antimicrobial peptide resistance mechanisms of human bacterial pathogens. *Curr Issues Mol Biol* **8:** 11–26.

Olivot, J.M., Labreuche, J., Mahagne, M.H., Aiach, M., and Amarenco, P. (2006) Endogenous tissue-type plasminogen activator and cardioembolic brain infarct subtype. *J Thromb Haemost* **4:** 2513–2514.

Petersen, T.N., Brunak, S., von Heijne, G., and Nielsen, H. (2011) SignalP 4.0: discriminating signal peptides from transmembrane regions. *Nat Methods* **8:** 785–786.

Punta, M., Coggill, P.C., Eberhardt, R.Y., Mistry, J., Tate, J., Boursnell, C., *et al*. (2012) The Pfam protein families database. *Nucleic Acids Res* **40:** D290–D301.

Quevillon, E., Silventoinen, V., Pillai, S., Harte, N., Mulder, N., Apweiler, R., and Lopez, R. (2005) InterProScan: protein domains identifier. *Nucleic Acids Res* **33:** W116–W120.

Rahman, O., Cummings, S.P., Harrington, D.J., and Sutcliffe, I.C. (2008) Methods for the bioinformatic identification of bacterial lipoproteins encoded in the genomes of Grampositive bacteria. *World J Microbiol Biotechnol* **24:** 2377– 2382.

Rawlings, N.D., Barrett, A.J., and Bateman, A. (2012) MEROPS: the database of proteolytic enzymes, their substrates and inhibitors. *Nucleic Acids Res* **40:** D343–D350. Remmert, M., Linke, D., Lupas, A.N., and Soding, J. (2009) HHomp – prediction and classification of outer membrane proteins. *Nucleic Acids Res* **37:** W446–W451.

Rompikuntal, P.K., Thay, B., Khan, M.K., Alanko, J., Penttinen, A.M., Asikainen, S., *et al*. (2012) Perinuclear localization of internalized outer membrane vesicles carrying active cytolethal distending toxin from *Aggregatibacter actinomycetemcomitans*. *Infect Immun* **80:** 31–42.

Rose, R.W., Bruser, T., Kissinger, J.C., and Pohlschroder, M. (2002) Adaptation of protein secretion to extremely highsalt conditions by extensive use of the twin-arginine translocation pathway. *Mol Microbiol* **45:** 943–950.

Sawabe, T., Ogura, Y., Matsumura, Y., Feng, G., Amin, A.R., Mino, S., *et al*. (2013) Updating the Vibrio clades defined by multilocus sequence phylogeny: proposal of eight new clades, and the description of *Vibrio tritonius* sp. nov. *Front Microbiol* **4:** 414.

Schmitt, P., Duperthuy, M., Montagnani, C., Bachère, E., and Destoumieux-Garzón, D. (2011) Immune responses in the Pacific oyster *Crassostrea gigas*. An overview with focus on summer mortalities. In *Oysters: Physiology, Ecological Distribution and Mortality*. Qin, J. (ed.). New York, USA: Nova Science Publishers Inc, pp. 227–273.

Schmitt, P., Rosa, R.D., Duperthuy, M., de Lorgeril, J., Bachere, E., and Destoumieux-Garzon, D. (2012) The antimicrobial defense of the Pacific oyster, *Crassostrea gigas*. How diversity may

compensate for scarcity in the regulation of resident/pathogenic microflora. *Front Microbiol* **3:** 160.

Shinoda, S., and Miyoshi, S. (2011) Proteases produced by vibrios. *Biocontrol Sci* **16:** 1–11.

Sikora, A.E., Zielke, R.A., Lawrence, D.A., Andrews, P.C., and Sandkvist, M. (2011) Proteomic analysis of the *Vibrio cholerae* type II secretome reveals new proteins, including three related serine proteases. *J Biol Chem* **286:** 16555– 16566.

Tomarelli, R.M., Charney, J., and Harding, M.L. (1949) The use of azoalbumin as a substrate in the colorimetric determination or peptic and tryptic activity. *J Lab Clin Med* **34:** 428–433.

Tusnady, G.E., and Simon, I. (2001) The HMMTOP transmembrane topology prediction server. *Bioinformatics* **17:** 849–850.

Vallenet, D., Belda, E., Calteau, A., Cruveiller, S., Engelen, S., Lajus, A., *et al*. (2013) MicroScope – an integrated microbial resource for the curation and comparative analysis of genomic and metabolic data. *Nucleic Acids Res* **41:** D636–D647.

Wai, S.N., Takade, A., and Amako, K. (1995) The release of outer membrane vesicles from the strains of enterotoxigenic *Escherichia coli*. *Microbiol Immunol* **39:** 451–456.

Wai, S.N., Lindmark, B., Soderblom, T., Takade, A., Westermark, M., Oscarsson, J., *et al*. (2003) Vesiclemediated export and assembly of pore-forming oligomers of the enterobacterial ClyA cytotoxin. *Cell* **115:** 25–35.

Yozwiak, M.L., and Songer, J.G. (1993) Effect of *Corynebacterium pseudotuberculosis* phospholipase D on viability and chemotactic responses of ovine neutrophils. *Am J Vet Res* **54:** 392–397.

Yu, C.S., Chen, Y.C., Lu, C.H., and Hwang, J.K. (2006) Prediction of protein subcellular localization. *Proteins* **64:** 643– 651.

Yu, N.Y., Wagner, J.R., Laird, M.R., Melli, G., Rey, S., Lo, R., *et al*. (2010) PSORTb 3.0: improved protein subcellular localization prediction with refined localization subcategories and predictive capabilities for all prokaryotes. *Bioinformatics* **26:** 1608–1615.

Zhang, X.H., and Austin, B. (2005) Haemolysins in *Vibrio* species. *J Appl Microbiol* **98:** 1011–1019.

Tables and Figures

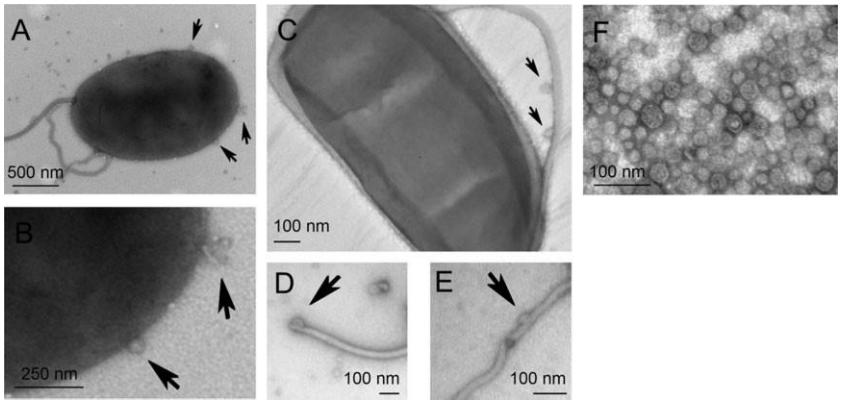

FIGURE 1. *Vibrio tasmaniensis* LGP32 secretes outer membrane vesicles.
A–E. Transmission electron microscopy of negatively stained LGP32 cultures in logarithmic phase of growth. Extracellular vesicles produced by LGP32 (black arrows) are observed detaching from outer membrane (A–B) or from the polar flagellum (C–E).
B. Enlarged part of the picture A.
F. Transmission electron microscopy of negatively stained vesicles obtained by ultracentrifugation. The vesicle diameters range from 30 to 50 nm

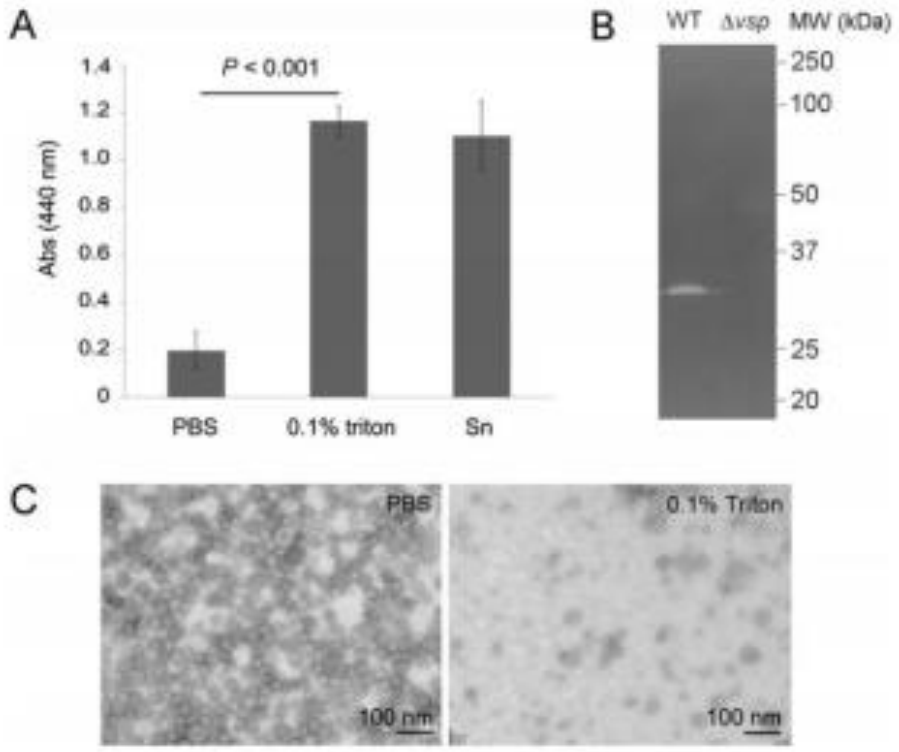

FIGURE 2. Proteases are encapsulated in LGP32 OMVs.

A. Protease activity was determined by azocasein hydrolysis (absorbance 440 nm) on 1 mg ml−1 ultracentrifuged supernatant of LGP32 ECPs (Sn) as well as on 2 mg ml−1 OMVs from LGP32 lysed in 0.1% Triton X-100 or resuspended in PBS (intact OMVs). Data were generated from three independent ECPs preparations. Data are the mean of three independent OMVs production + /− SEM.

B. Zymography showing gelatin hydrolysis (clear zone) by OMVs preparations from wild-type and Δvsp LGP32 vibrios. Molecular masses are indicated on the right.

C. Transmission electron microscopy of negatively stained vesicles resuspended in PBS (intact) or lysed in 0.1% Triton X-100.

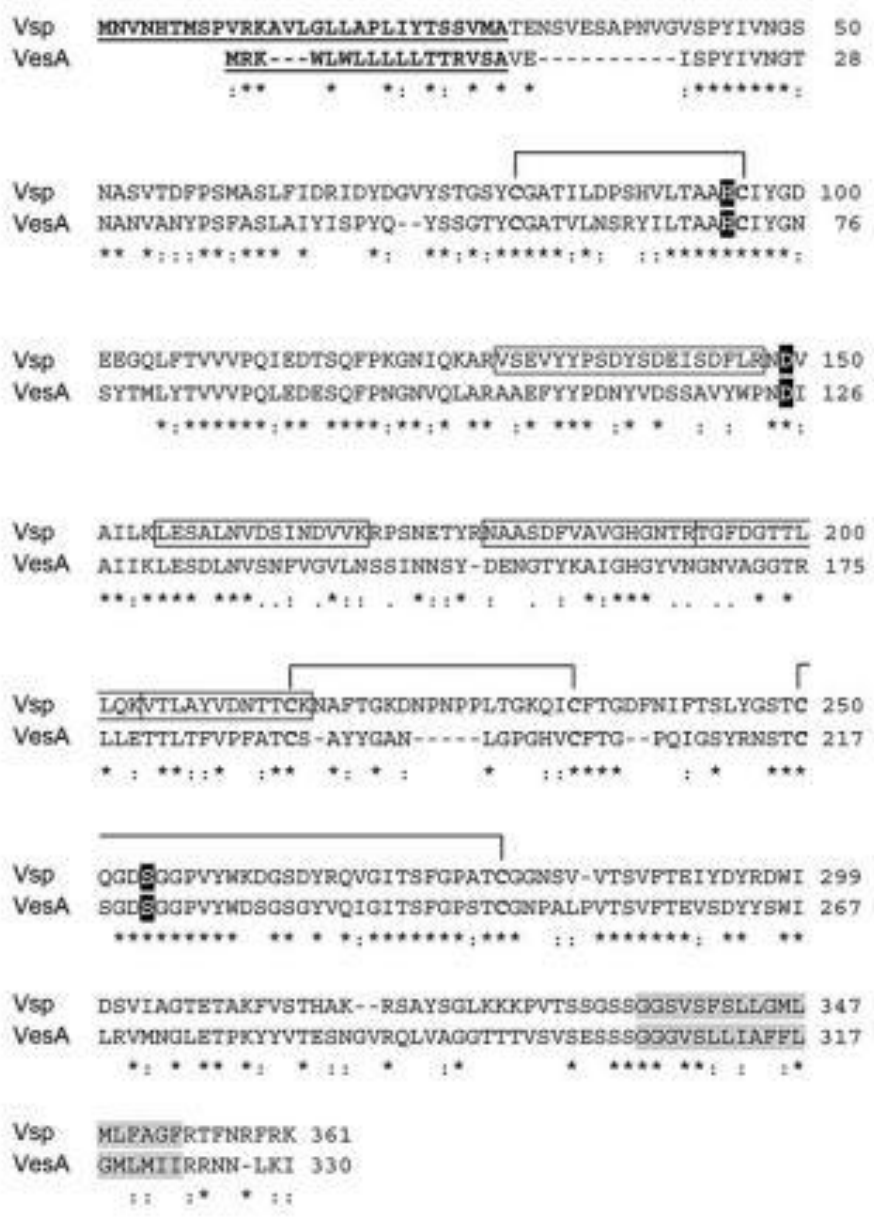

FIGURE 3. The intravesicular Vsp protease is a homologue of the serine protease VesA.
Peptides identified by MS-MS sequencing after trypsin digestion of the zymography active band (boxes) are displayed on the amino acid sequence deduced from the VS_II0815 (Vsp) nucleic acid sequence. The sequences of LGP32 Vsp and Vibrio cholera VesA (VCA0803) were aligned with ClustalW. Identical amino acids are indicated by an asterisk. Conservative replacements are indicated by a colon. Conserved amino acids involved in the catalytic triad of serine proteases (His95, Asp149, Ser254) are highlighted in black. Conserved positions of predicted cysteine bridges are indicated with hooks. The predicted signal peptides are underlined. The transmembrane helices predicted with Phobius and TMHMM are highlighted in grey. Amino acids are numbered on the right.

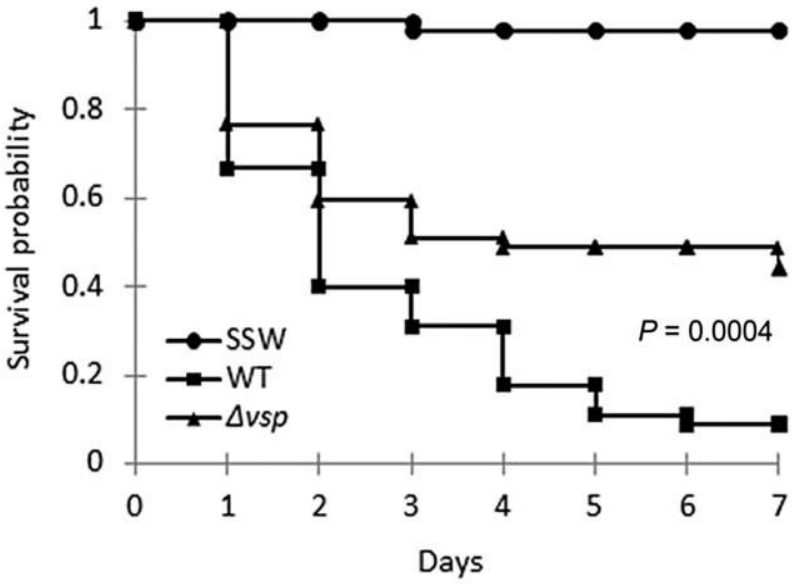

FIGURE 4. The virulence of the Δ*vsp* mutant is attenuated in oyster experimental infections. Kaplan–Meier survival curves from oyster infection experiments. Juvenile oyster were injected with 4×10^7 cfu per animal of the wild-type LGP32 (square) or the isogenic Δ*vsp* (triangle) mutant. An injection of sterile seawater (SSW) was used as control (circle). Groups of 45 oysters (15 per seawater tank) were monitored for 7 days after infection. Data are representative of two independent experiments

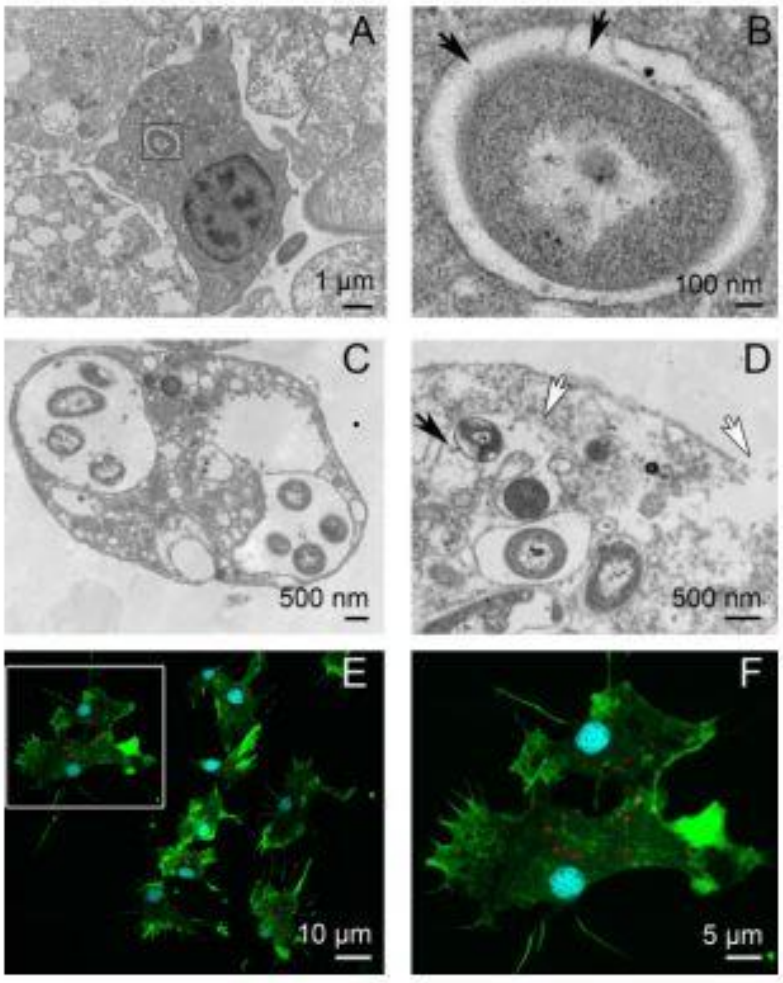

FIGURE. 5. Intracellular and extracellular delivery of OMVs to oysterimmune cells.

A and C. MET observation of oyster haemocytes containing intraphagosomal LGP32 after phagocytosis (30 min contact).

A. Two intracellular LGP32 are observed together with one extracellular LGP32. The haemocyte does not show any evidence of cell damage.

B. Enlarged part of the picture in A showing the release of OMVs by intraphagosomal LGP32 (black arrows).

C–D. Oyster haemocytes containing numerous intracellular LGP32 display major alterations including loss of organelle integrity and damages to the cytoplasmic and the phagosomal membranes (white arrows).

E. Confocal microscopy section showing the internalization of PKH26-labeled OMVs (red) by most haemocytes after 2 h of incubation in vitro (white arrows). Haemocyte nuclei were stained with DAPI (blue).

F-actin was stained with phalloidin (green). F. Enlarged part of the picture in C showing the intracellular localization of PKH26-labeled OMVs.

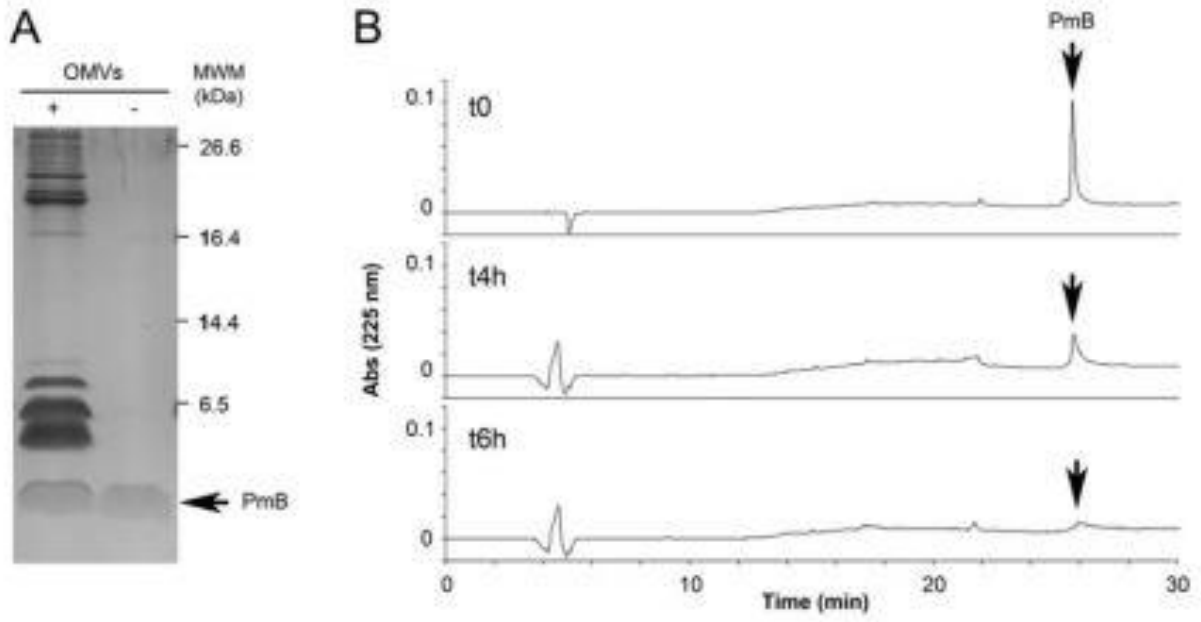

FIGURE. 6. Polymyxin B is titrated but not degraded by V. splendidus LGP32 OMVs.

A. Silver-stained Tris-Tricine SDS-PAGE of PmB (0.6 µg) incubated for 6 h in the presence (+)/absence (−) of 2 µg OMVs. Molecular masses (kDa) are shown on the right.

B. Time-course of PmB titration by wild-type OMVs monitored by RP-HPLC. PmB (30 µg) was incubated with 100 µg OMVs. The PmB trace (arrow) was monitored at 0, 4 and 6 h on a UP5-ODB-25QS column using a 0–70% acetonitrile gradient over 35 min.

Strain	OMVs (μg ml^{-1})		MIC of PmB (μM)
	Wild-type	Δ*vsp*	
Wild-type LGP32	0	0	0.78
Wild-type LGP32	6.25	0	1.56
Wild-type LGP32	12.5	0	3.12
Wild-type LGP32	25	0	6.25
Wild-type LGP32	50	0	12.5
Wild-type LGP32	0	50	12.5
Δ*vsp* LGP32	0	0	0.78

TABLE 1. Minimum inhibitory concentration (MIC) of polymyxin B in the presence/absence of OMVs from wild-type and Δvsp LGP32.

Supporting information

Fig. S1. The major protease of OMVs is not the major extracellular metalloprotease Vsm. Characterization of the protease activity associated to OMVs. Zymography showing gelatin hydrolysis by OMVs (pellets, 5 µg) or ultracentrifuge supernatants (5 or 0.1 µg) from the wild-type and Δ*vsm* LGP32. Molecular masses (kDa) are shown on the left. The active band of wild-type OMVs is maintained in the Δ*vsm* mutant. No band at the same molecular mass is visible in ultracentrifuge supernatants of the WT and Δ*vsm* mutant.

Fig. S2. Vsp activity is stable in a pH range of 5.6 to 7.7. Zymography showing gelatin hydrolysis by OMVs from the wild-type LGP32 (10 µg) at 20°C and 37°C in 50 mM citrate buffer pH 4.4 or 50 mM phosphate buffer pH 5.6, 6.8 and 7.7. Molecular masses are shown on the right.

Fig. S3. Effect of plasma on LGP32 growth and OMV production. (A) Growth curves of wild-type (WT) LGP32 (black) and its isogenic Δ*vsp* mutant (white) were obtained in Zobell medium (squares) and oyster plasma (circles) at a temperature of 20°C. Culture turbidity was monitored at 600 nm every 1 h. The *vsp* deletion did not impair growth of LGP32 in Zobell medium nor in plasma. (B–C) Transmission electron microscopy of negatively stained wild-type LGP32 cultures in Zobell medium (B) and filtered oyster plasma (C). While only few OMVs were released in Zobell medium (A), a massive release of OMVs was observed in plasma (B).

Fig. S4. Control of *vsp* gene deletion.

A. PCR amplification of the DNA region flanking the *vsp* gene. DNA extracted from the wild-type (WT) and the three Δ*vsp* mutants (1, 2, 3) was amplified using the VS_II0815-Fw2 and VS_II0815-Rv2 external primers (Supporting Information Table S3). The molecular weight marker is displayed on the left. The expected size for the wild-type and Δ*vsp* amplicon are 2111 bp and 1025 bp respectively.

B. Control of *vsp* deletion by sequencing. The PCR-amplified fragments obtained from the Δ*vsp* 1, 2 and 3 mutants were sequenced. Sequences were aligned with that of wild-type LGP32 using ClustalW. Gaps corresponding to the deletion are indicated by dashes. The VS_II0815-Fw2 and VS_II0815Rv2 primers used for sequencing are underlined. The ATG and stop codons of the *vsp* open-reading frame are displayed in white and grey boxes respectively.

Fig. S5. Attenuated virulence of two additional Δ*vsp* mutants is in oyster experimental infections. Kaplan–Meier survival curves were generated from 45 juvenile (A) or adult (B) oysters injected with wild-type (square) or Δ*vsp* (triangle) LGP32 (4×10^7 cfu per juvenile oyster or 2×10^8 cfu per adult oyster). An injection of sterile seawater (SSW) was used as control (circle). Two Δ*vsp* mutants obtained independently were used in experimental infections (A) and (B). Oysters (15 per seawater tank) were monitored for 7 days after infection.

Table S1. List of proteins associated to *V. splendidus* LGP32 OMVs.
Protein identification was carried out by comparing experimentally generated monoisotopic peaks of peptides with computer-generated fingerprints using the Mascot program. Mascot was run on protein sequences deduced from four sequenced *V. splendidus* LGP32 genome (Le Roux *et al*., 2009). Only proteins identified by more than three peptides in two independent OMV preparations are displayed. OMV prep #1 was crude while OMV prep #2 was purified by density gradient. Only proteins found in both preparations are displayed. P, M, N and L stand for protease, murein hydrolase, nuclease and lipase respectively. OM and IM stand for outer and inner membrane respectively. The Vsp line is displayed in boldface.

Table S2. Molecular functions associated to OMV proteins. Two independent OMV preparations were compared: OMV prep #1 was crude while the OMV prep #2 was purified on density gradient. The numbers of proteins assigned to a given molecular function are similar in both preparations. The molecular functions associated to the 132 proteins common to OMV prep #1 and #2 (detailed in Supporting Information Table S1) are shown on the right column.

Table S3. Strains, plasmids and oligonucleotides.